DESIGN AND EVALUATION OF A POLYIMIDE SPRING SYSTEM FOR THE SCANNING FORCE MICROSCOPE OF THE PHOENIX MARS MISSION 2007

D. Parrat[(1)], S. Gautsch [(1)], L. Howald[(2)], D. Brändlin-Müller[(2)], N. F. De Rooij[(1)] and U. Staufer[(1)]

[(1)]Institute of Microtechnology (IMT), University of Neuchâtel, Jaquet-Droz 1, 2007 Neuchâtel, Switzerland, Email: urs.staufer@unine.ch (corresponding author)
[(2)] Nanosurf AG, Grammetstrasse 14, 4410 Liestal, Switzerland, Email: howald@nanosurf.com

ABSTRACT

Precise motions in the nanometer and Angstrom range can be achieved by magnetic forces, deflecting a spring mounted platform. Permanent magnets, which are mounted on that platform, are either attracted or repelled by magnetic fields, which are generated in rigidly mounted coils underneath the magnets. These electro-magnetic forces are counter-balanced by mechanical springs, which suspend the platform from the same rigid frame to which the coils are mounted. Rapid actuation may cause mechanical ringing if such a stage is not properly damped. We have evaluated internal friction of the springs as damping mechanism. We found that polyimide springs provide two to three times better damping and moderate temperature dependence compared one made of stainless steel. This allowed us increasing the scan speed of an AFM by a factor of more than two.

1. INTRODUCTION

In April 2001, NASA's Mars Surveyor Lander (MSL), conceived to realize several in-situ experiments on Mars, was ready to be launched, but was cancelled due to the back to back loss of two NASA missions at the end of 1999, Mars Climate Orbiter (MCO) and Mars Polar Lander (MPL). One instrument suite on the MSL called MECA (for Microscopy, Electrochemistry and Conductivity Analyzer) was foreseen to measure among other properties the size, its distribution, and the shape of dust and soil particles on Mars, aiming at understanding the seasonal variation of the Martian climate as well as the geological and hydrological history of the planet. An AFM, dubbed FAMARS (for "First AFM on Mars"), in combination with an optical microscope enabled imaging particles from millimeters to nanometers in size [1, 2, 3].

After cancellation of the mission, the MECA consortium sought for a new flight opportunity by joining the PHOENIX project in a competition for the first Scout mission to Mars, announced by NASA in 2002. The Phoenix mission was selected, and MECA will see its second chance for a journey to Mars onboard of the 2007 Lander. This mission will integrate scientific instruments from MPL and MSL. The goal of the mission is to perform a scientific analysis of the Martian arctic soil for clues to its history of water and geology and the potential for biology.

Even though the first flight was cancelled, the instrument had been successfully characterized and measurements of particles in Mars equivalent conditions had been accomplished [3, 4].

One problem of the first FAMARS design occurred at low temperatures: We had planed to use grease for mechanically damping the scanning motion, a method which had proofed to be successful for laboratory applications. However, at the large span of operation temperatures expected to be encountered on Mars, the viscosity of all available greases or oils varied too much, which caused intolerable scan field distortions. The only remedy was to operate FAMARS without damping and consequently at significantly reduced scan speeds.

In this article, we present modifications performed on this first generation of FAMARS (referred now as FAMARS 1) to overcome this problem. In particular, we describe a polyimide spring system designed and fabricated for the new AFM, dubbed FAMARS 2. Section 4 then reports about AFM measurements and environmental testing performed with the new design.

2. DESCRIPTION OF FAMARS 1

Volume, weight and power consumption are critical design parameters for instruments to be applied in space missions. For this reason, the x-y-z scanner of FAMARS 1, shown in Fig.1, measured 12 mm x 18 mm x 24 mm and weighted only 15 g. The power consumption of the whole microscope was less than 8.5 W.

The AFM consisted of three distinctive parts: a micro-fabricated cantilever sensor chip made of silicon and shown in Fig. 2, an electromagnetic scanner, and the controller electronics. Maximum functionality was transferred to the micro-fabricated silicon chip. A stress sensor was integrated into each silicon

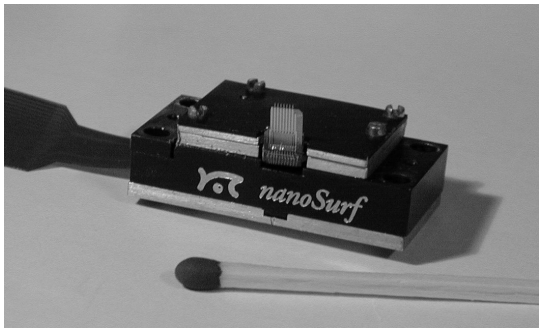

Fig. 1. FAMARS 1 scanner with a cantilever sensor chip mounted on it.

cantilever. Swapping out of a blunt or contaminated tip, or a broken cantilever was achieved by using an array of eight cantilevers in the following manor: The array was mounted with two tilt angles, thus only one tip at the time was in contact with the sample during imaging. Each cantilever was located at the end of a thick support beam that could be cleaved off in case the cantilever was no longer usable. Moving the chip closer to the sample then brought the next tip into a measuring position.

In standard AFM designs, piezo-ceramic actuators are used for scanning areas of several tens of micrometers. These actuators require driving voltages of more than 100 V for such large strokes. This type of actuation can become problematic due to the risk of arcing in the Martian CO_2 atmosphere of 0.7 mbar. A further drawback is the size of large stroke piezo actuators. A different technique based on electromagnetic actuation was therefore employed, reducing the potentials of the driving signals to 12 V. This scanning principle is illustrated in Fig. 3. Three permanent magnets were

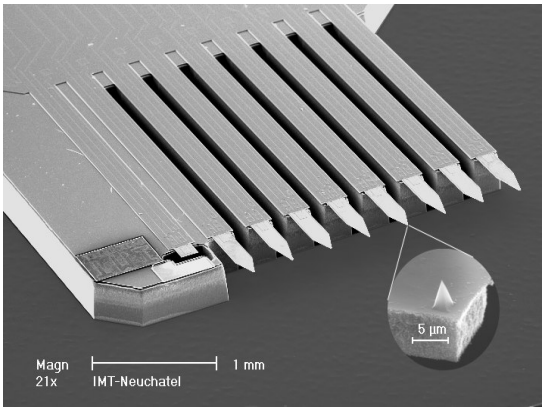

Fig. 2. FAMARS chip. The cantilever on the right is the first to be used. A silicon tip is located at the end of each cantilever.

attached to a spring-suspended platform. Underneath of each magnet, a coil was rigidly attached to the body of the scanner, which allowed exerting a force on the magnet above it by passing a current through it. The suspension system had to be critically damped in order to allow fast movements without ringing. Damping is inversely proportional to the quality factor Q of a spring. As the springs were made of stainless steel, having a high quality factor, special grease (Apiezon® N) was applied to them for increasing the loss of energy, i.e. for damping.

The AFM sensor-chip was mounted on the platform and, hence, several (13) electrical contacts needed to be fed to it. This was performed by a flexprint circuit, which connected the chip and the coils to the electronic board. To connect the chip, the flexprint was glued on the backside of the suspended platform. To avoid constraining the platform, the flexprint was cut at the interface between the platform and the fixed part of the scanner. Then, thin and soft wires were added to reconnect the copper lines.

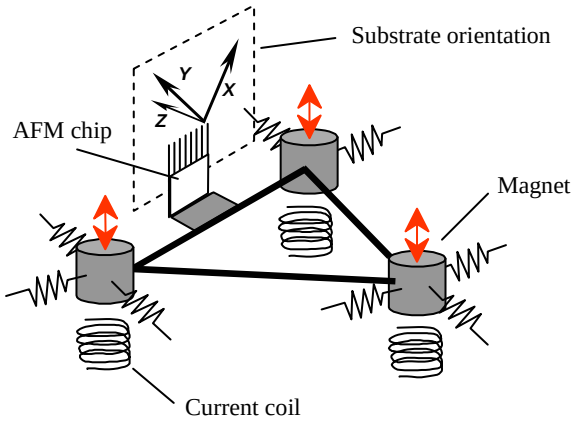

Fig. 3. FAMARS scanning principle

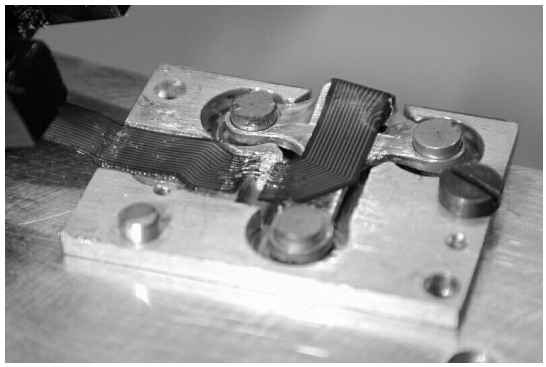

Fig. 4. Backside view of the platform of FAMARS 1. The flexprint was cut at the interface and wire bonding was then employed for reconnecting the copper lines.

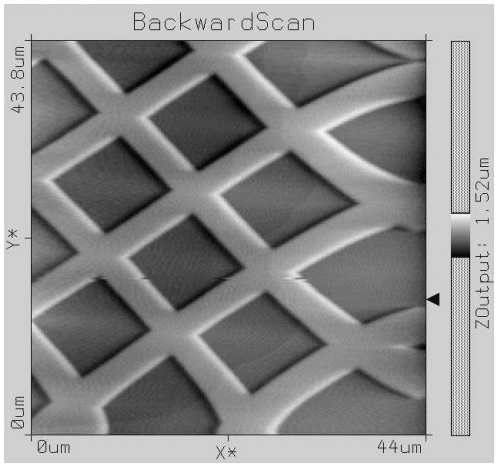

Fig. 5. Image of a calibration grid taken by means of FAMARS 1 at 0°C. The distortion due to the damping grease is visible at the beginning of each scan line.

At temperatures below 0°C, the viscosity of the grease increased, causing distortions in the scan field, especially at the beginning of each scan line (see Fig. 4.) [3]. This effect was even stronger at lower temperatures; the grease became so stiff that no movement was possible anymore.

The only short term solution to this problem was to run the scanner without grease. The vibrations of the platform due to the reduced damping were transmitted to the cantilevers. This was particularly true under Mars equivalent pressure (7 mbar), where also the surrounding gas could not provide useful damping. Interferences with these vibrations could be reduced by adjusting the feedback loop settings and by significantly reducing the scan speed.

3. NEW DESIGN AND FABRICATION

As an alternative to viscous damping, internal friction inside the springs themselves was considered. An attractive material for that purpose is polyimide since compared to stainless steel it is a lossy material, it is space compatible and it can be used as flexible printed-board, allowing integrating the electrical leads to the scanner into the suspension springs. First we compared various types of polyimide with stainless steel, to evaluate and compare their relative damping properties.

3.1 Preliminary measurements on polyimides

The damping constant of a material, also called internal friction, is equal to Q^{-1}, where Q is the quality factor of a mechanical resonator made of this material. Q is equal to the ratio of the resonance frequency f_0 to the half-width Δf of the respective resonance curve.

$$Q = \frac{f_0}{\Delta f} \qquad (1)$$

We measured the quality factor Q for different beams made of polyimide or stainless steel (see Table 1.). We investigated the properties of the flexprint already present in the FAMARS 1 design, composed of two layers of polyimide (Kapton® with copper lines in-between), plain Kapton (without copper film), and UPISEL®-N (another flexible, copper clad laminate, based on the polyimide UPILEX®-VT).

The beams were vibrated by means of a piezoelectric actuator. A liquid nitrogen circuit allowed varying the temperature between 20°C and -50°C, and a laser interferometer recorded the deflection of the beams. The results were as expected and are summarized in Table 2.

Polyimides showed a lower quality factor than stainless steel, i.e. a higher damping constant. While the damping for UPISEL-N was about two times higher than that of stainless steel, it was about three times higher for Kapton, which was expected because of the higher flexibility of Kapton. For the flexprint, essentially composed of Kapton, the damping was even higher. We attribute this to the additional friction between the copper lines and the two Kapton layers.

The results for Kapton and the flexprint are represented in more detail in Fig. 6. Contrary to Kapton, which is

Table 1. Materials whose quality factor was determined during preliminary tests.

Material	Thickness
Stainless steel 1.4310	50 µm
Kapton® 300 HN (DuPont)	75 µm
Flexprint	250 µm
UPISEL®-N SE 1320 (Ube Industries)	50 µm UPILEX-VT + 12 µm Cu

Table 2. Quality factors of the tested materials for temperatures between -50°C and +20°C.

Material	Quality factor
Stainless steel 1.4310	100-220
Kapton® 300 HN	40-45
Flexprint	26-38
UPISEL®-N SE 1320	60-63

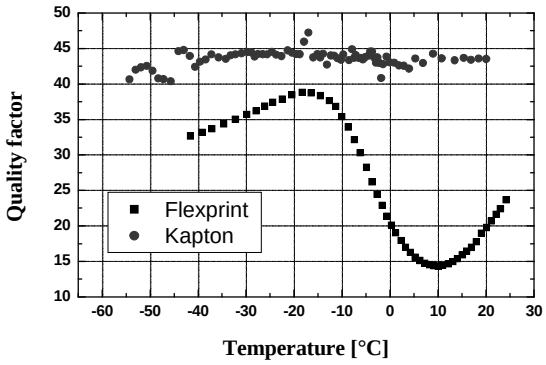

Fig. 6. Quality factor curves for Kapton and the flexprint.

known for its stable properties on a wide range of temperature, the flexprint showed a variation in damping, which we attribute to the copper. Moreover, we saw that the bimorph effect caused considerable bending of the beam at low temperature.

These first data indicated that Kapton, as a material for the springs, could improve the damping of the system. The damping was even higher with the flexprint; however, the bimorph effect must be avoided in the respective new spring design.

3.2 FAMARS 2 design

A new spring system was conceived in a flexprint compound. For avoiding the bimorph effect, the flexprint leaf was symmetrically designed: copper lines are deposited on each side of a 50 µm layer of Kapton. Two 25 µm cover layers protect these lines (see Fig. 7).

The flexprint was structured by laser cutting; the minimal dimension was the width of the spring's branches, which was 360 µm. The dimensions of the branches were designed to have the same stiffness than that of FAMARS 1.

Fig. 7. Schematic view of the flexprint.
a) Kapton layer, thickness 50 µm
b) Copper lines, thickness 5 µm
c) Kapton layer, thickness 25 µm

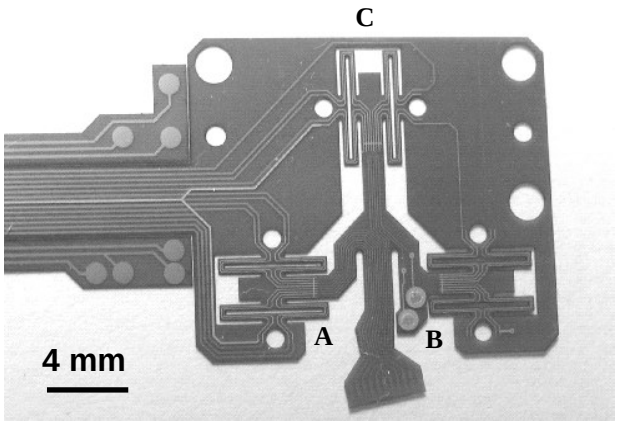

Fig. 8. View of the flexprint prior to mounting to the scanner-head. The two springs at the bottom (A, B) are the x-spring and y-spring and the upper one (C) z-spring respectively.

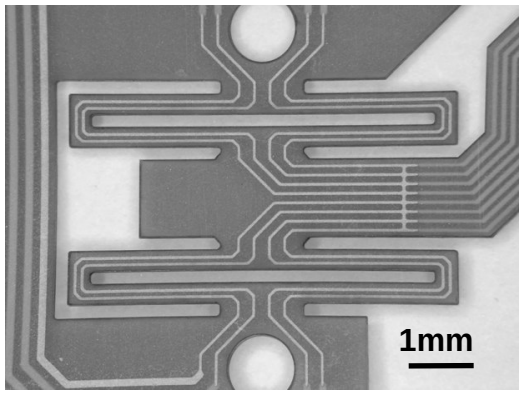

Fig. 9. View of the x-spring. The copper lines on the visible side were designed for compensating the bimorph effect. The electrical connections were established by the copper lines on the hidden side.

Changing the flexprint design induced small modifications in the others parts as well. These where minor changes for adapting the form factor and are not further detailed here. After assembly, all external dimensions and the total weight were kept constant compared to FAMARS 1. Figure 10 shows the FAMARS 2 scanner without cover, allowing to see the flexprint leaf sandwiched between two aluminum plates.

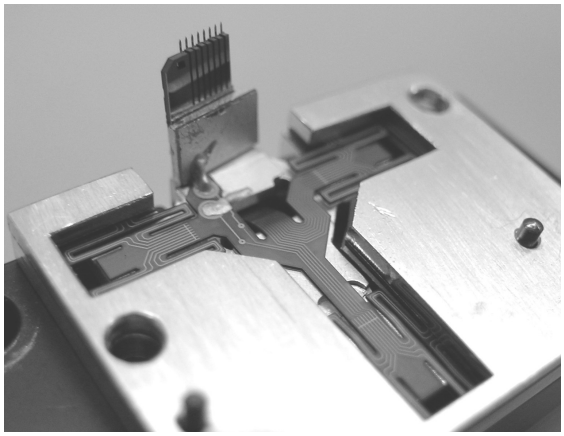

Fig. 10. FAMARS 2 scanner without cover. The platform was suspended by the three Kapton springs. Magnets were glued under the platform. This view corresponds to the schematic drawing of Fig. 3.

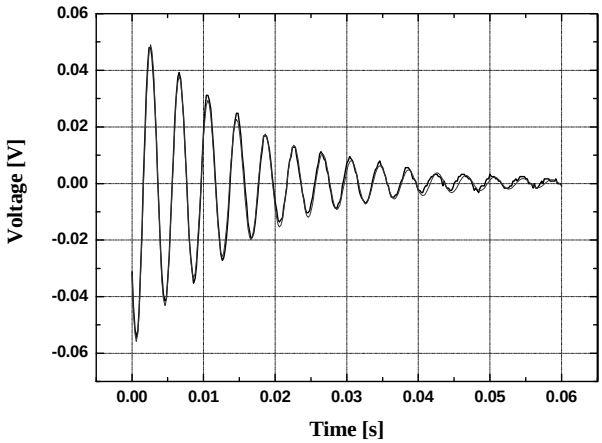

Fig. 11. Recording of the decreasing voltage on the z-coil of FAMARS 1 at 20°C. It allowed us determining t_0, by fitting it with the function described in Eq. 3.

4. EXPERIMENTS

Testing of the new spring system was performed in several steps. First, we measured the damping properties of the springs at the operation temperatures in order to confirm the preliminary measurements conducted with plain polyimide. Then AFM images were taken, and finally the scanner was exposed to various environmental conditions for space qualification.

4.0 Damping measurements

For characterizing the springs, we measured the decay time t_0, which is the time during which the amplitude of a free oscillation decays to 1/e of its initial value. Eq. 2 shows the relation between Q and t_0, where t_0 also depends on the resonance frequency ω of the system.

$$t_0 = \frac{Q}{\pi\omega} \qquad (2)$$

For measuring t_0, we applied a DC current to the three coils, to deflect the platform to its highest position. Then, we simultaneously switch off all currents, forcing a step-like displacement of the platform. Due to the motion of the magnets, a secondary current was induced in the coils. This current was converted into a voltage and measured for determining t_0, by fitting it with the function described by Eq. 3.

$$V(t) = V_0 \cdot e^{-\frac{t}{t_0}} \sin\left(\pi \frac{t - t_c}{w}\right) \qquad (3)$$

We did these measurements for FAMARS 1 (with and without grease on the springs) and for FAMARS 2 at the operation temperatures. Fig. 11 shows the results for the z-spring of FAMARS 1 at 20°C. The matching between the curve and the fit is so good that the two can hardly be distinguished on that graph.

The results for the z-springs of FAMARS 1 and FAMARS 2 are shown in Fig. 12. We observed that the damping is about two times higher for FAMARS 2 than for FAMARS 1 without grease. For FAMARS 1 with grease, the damping is very high at ambient temperature, but the stiffness of the grease hindered the platform to move at low temperatures. Note that the curve for FAMARS 2 has its maximum at about -20°C and its minimum at about +10°C, like the curve for Q that we had obtained for the flexprint beam (see Fig. 6). The flexprint springs had therefore a better damping than those made of stainless steel, if no grease was applied to them.

4.1 AFM Measurements

The damping of FAMARS 2 was encouraging, so we performed AFM measurements to determine the properties of the new scanner. The main parameter to evaluate was the maximal scan area, referred as scan range. Imaging also provided quantitative information for the improvement of the damping in terms of scan speed.

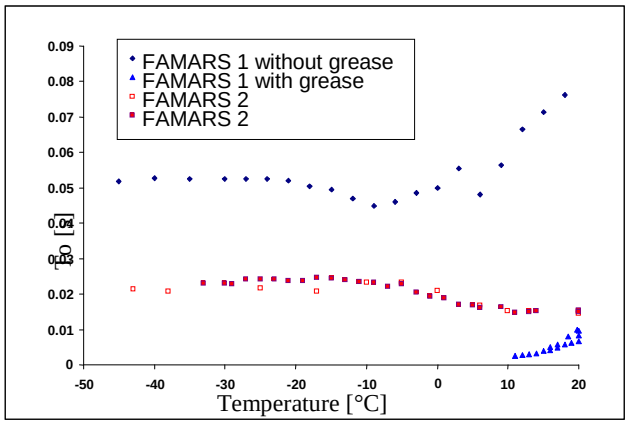

Fig. 12. Decay time t_0 of the z-spring of FAMARS 1 and FAMARS 2. t_0 is lower for FAMARS 2 than for FAMARS 1 without grease. t_0 for FAMARS 1 with grease shows the best damping at ambient temperature, but the stiffness of the grease blocks the springs at temperatures below 10°C.

For evaluating the scan range, we used an orthogonal grid in silicon with known height and period. The grid had a step height of 200 nm and a pitch of 10 µm.

Images were performed in both static and dynamic mode at temperatures between -30°C to +30°C.

4.2 Environmental and fatigue testing

Environmental tests helped us to determine if the instrument will be robust enough to handle the extreme conditions in space and space travel.

First, vibrations tests were performed to determine the resistance of the scanner to the launch conditions. The scanner was tested along its three axes, with a vibration spectrum (see Fig. 13) corresponding to the launch vibrations. Figure 14 shows FAMARS 2 mounted on the vibration-test table. A holder in aluminum was used to fix the AFM in the same position as that in the MECA instrument suite.

Shock tests are currently in progress, and thermal cycles will be performed in near future.

Fatigue test were also performed by applying an AC current to the three coils during several days, in order to know the behavior of the platform after a large number of oscillations.

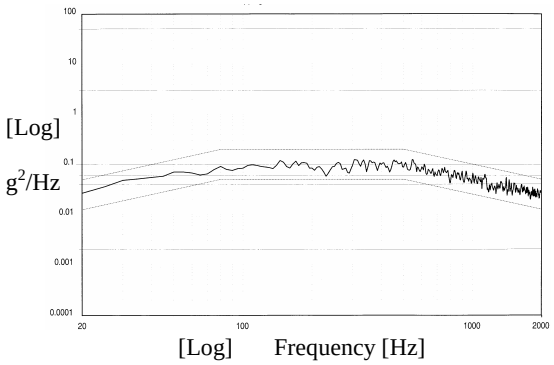

Fig 13. Random vibration spectrum encountered by FAMARS 2 along the z-axis. Spectra along x-axis and y- axis were similar.

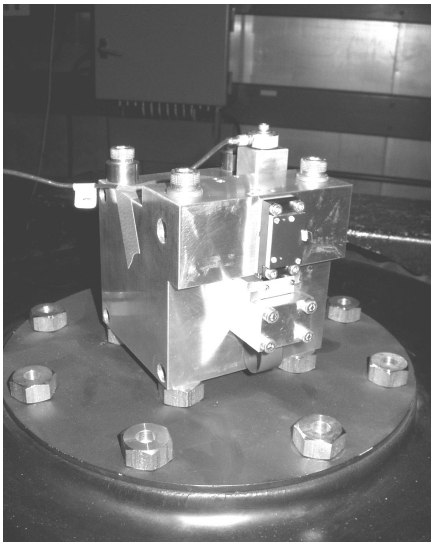

Fig. 14. FAMARS 2 mounted on the vibration-test table. An accelerometer is located at the top of the aluminum holder for recording the vibrations spectrum.

5. RESULTS

5.1 AFM Measurements

The grid was successfully imaged in both static and dynamic modes. Due to the scanning principle, the scan field was never perfectly planar but described by a "saddle" like shape. This phenomenon has been observed already with FAMARS 1, and could be corrected by using a planar fit algorithm.

Fig. 15 shows four images of the calibration grid taken at different temperatures. The distortion was comparable to that observed with FAMARS 1 at room temperature. The squares were not orthogonal, but this could be corrected by adjusting several parameters in the software that drove the scanner. By keeping the

same parameters for these four images, we saw a reduction in the scan area of about 30% from 30°C to -25°C. This meant that the stiffness of the springs became higher at lower temperature. This could be a drawback of the new spring system, if the scan range becomes smaller than the required forty micrometers.

The time necessary to take these images was ten minutes for each image. Compared to FAMARS 1, where this had taken twenty-five minutes, the savings in time were significant.

5.2 Environmental and fatigue testing

After the vibration tests, the chip and the scanner were still intact. AFM measurements were performed to insure that the behavior of the scanner was the same. No significant changes in the calibration parameters were observed, showing that FAMARS 2 could withstand the vibrations test.

For the fatigue test, FAMARS 2 stage was deflected for more than hundred millions of oscillations at ambient temperature and ten millions at -50°C. The damping properties of the springs were still the same and no visible changes appeared on the springs.

6. CONCLUSION

We designed and fabricated a new spring system in polyimide for the FAMARS instrument. Due to the high damping of polyimide compared to stainless steel, the scan speed at low temperature was increased more than twice. The scanner passed fatigue and vibrations tests. Further tests for fully qualifying the scanner for space are in progress.

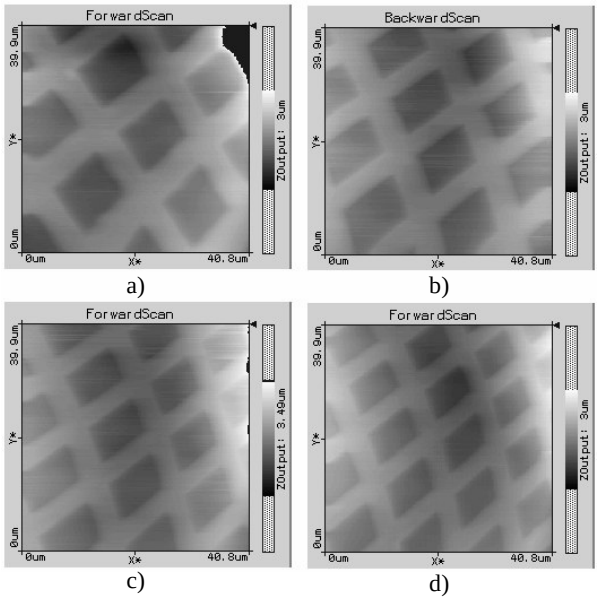

Fig. 15. AFM images in static mode of a calibration grid taken at a) -25°C, b) 10°C, c) 15°C and d) 30°C. At low temperature, the scan range was decreased.

7. AKNOWLEDGEMENTS

Helpful discussions with W.T. Pike (Imperial College, London, UK), M. Hecht, M. Shirbacheh, and C.T. Mogensen (JPL, Pasadena, USA) are acknowledged.

We thank the Canton of Neuchâtel, the Space Center at EPFL, and the Wolfermann-Nägeli Foundation for financial support.

8. REFERENCES

1. S. Gautsch, T. Akiyama, N.F. de Rooij, U. Staufer, Ph. Niedermann, L. Howald, D. Müller, A. Tonin, H.-R. Hidber, W.T. Pike and M.H. Hecht, "Atomic force microscope for planetary applications", *Solid-State Sensor and Actuator Workshop*, pp. 267-270, Hilton Head Island, USA, June 4-8, 2000.

2. W.T. Pike, M.H. Hecht, M.S. Anderson, T. Akiyama, S. Gautsch, N. F. de Rooj, U. Staufer, Ph. Neidermann, L. Howald, D. Müller, A. Tonin, and H.-R. Hidber, "Atomic Force Microscope for Imaging and Spectroscopy", *Concepts and Approaches for Mars Exploration*, [6200], Lunar and Planetary Institute, Houston, TX, July 18–20, 2000.

3. S. Gautsch, *Development of An Atomic Force Microscope and Measurement Concepts for Characterizing Martian Dust and Soil Particles*, PhD thesis, University of Neuchâtel, Switzerland, 2002.

4. S. Gautsch, T. Akiyama, R. Imer, N.F. de Rooij, U. Staufer, Ph. Niedermann, L. Howald, D. Brändlin, A. Tonin, H.-R. Hidber, W.T. Pike, "Measurement of Quartz Particles by Means of an Atomic Force Microscope for Planetary Exploration", *Surface and Interface Analysis*, 33, 163, 2000.